scientific reports

Check for updates

OPEN

Boric acid-functionalized bentonite nanostructures attenuated paraquat-induced pulmonary injuries in rats

Asma Talebian[1,6], Motahareh Soltani[2,6], Somayyeh Karami-Mohajeri[3,1]✉, Elham Jafari[4], Jafar Ahmadi[1], Mehdi Ranjbar[3]✉, Fatemeh Abedi[1] & Ali Mandegary[5]

This study evaluated the antioxidant, anti-inflammatory, and anti-fibrotic effects of boric acid-functionalized bentonite nanostructures (BABTs) in a rat model of paraquat (PQ)-induced pulmonary toxicity, a well-established model for herbicide-related lung fibrosis. BABTs (20–60 nm) were synthesized via a microwave-assisted technique, characterized by dynamic light scattering, scanning electron microscopy, Fourier-transform infrared, and ultraviolet–visible spectroscopy, confirming PQ-BABT complex formation. Forty-eight male Wistar rats were randomized into eight groups (n = 6/group): negative control (saline), positive control (single 100 mg/kg PQ oral dose), and experimental groups receiving BABTs or boric acid (BA) at 10, 50, or 100 mg/kg/day orally, 30 min post-PQ. After 14 days, lung malondialdehyde (MDA) levels and histopathological changes (H&E, Masson's Trichrome) were assessed. BABTs at 50 mg/kg significantly decreased lung malondialdehyde (MDA) levels ($P < 0.05$) and significantly attenuated tissue injury ($P < 0.05$), suggesting an attenuation of oxidative stress, inflammation, and fibrosis, while boric acid (BA) demonstrated no significant effect. BABTs mitigate PQ-induced lung injury through antioxidant, anti-inflammatory, and anti-fibrotic mechanisms, enhanced by reducing PQ bioavailability. These findings position BABTs as a promising therapeutic candidate for PQ-induced pulmonary fibrosis, warranting further clinical evaluation.

Keywords Paraquat, Pulmonary fibrosis, Boric acid, Functionalized bentonite nanostructures, Rat

Paraquat (PQ), also known as Gramoxone or methyl viologen, is a cationic, fast-acting, and non-selective quaternary nitrogen herbicide commonly used for its high effectiveness and minimal residue in crops[1,2]. However, PQ is highly toxic to humans and animals, contributing to significant annual mortality due to accidental or intentional ingestion, dermal exposure, or inhalation[3,4]. PQ is a multifunctional poison that affects several organs, including the liver, kidneys, heart, and central nervous system. But the most common and fatal injuries are lung damage and pulmonary fibrosis[3,4]. PQ accumulates in lung tissue, particularly in type II pneumocytes, via a selective, active polyamine uptake process[5,6]. The mechanisms underlying PQ toxicity are not fully understood. Oxidative stress, primarily driven by reactive oxygen species generation[2,7,8]. The reduction of PQ leads to the production of free radicals, causing oxidative damage, intra-alveolar fibrosis, and lung failure[9,10]. The lung injury caused by PQ leads to damage to alveolar epithelial cells (type I and II pneumocytes) and Clara cells, as well as disruptions to the surfactant system[1,2]. It also causes hemorrhage, edema, hypoxemia, infiltration of inflammatory cells into the interstitial and alveolar spaces, proliferation of fibroblasts, and excessive collagen deposition[11,12]. The high mortality rate of PQ-intoxicated patients poses a challenge for clinical practitioners due to the lack of an antidote or effective treatment to prevent these injuries[13]. Preventing the gastrointestinal absorption of toxins and reducing their bioavailability using chemical or natural adsorbents are among the detoxification strategies in the management of poisoning. Clays are composed of aluminum, magnesium, or

[1]Department of Toxicology and Pharmacology, Faculty of Pharmacy, Kerman University of Medical Sciences, Kerman, Iran. [2]Pistachio Safety Research Center, Rafsanjan University of Medical Sciences, Rafsanjan, Iran. [3]Pharmaceutical Research Center, Institute of Neuropharmacology, Faculty of Pharmacy, Kerman University of Medical Sciences, Kerman, Iran. [4]Pathology and Stem Cell Research Center, Department of Pathology, Faculty of Medicine, Kerman University of Medical Sciences, Kerman, Iran. [5]Traditional Pharmacy and Pharmaceutical Sciences Research Center, and Department of Pharmacology & Toxicology, Faculty of Pharmacy, Shahid Sadoughi University of Medical Sciences, Yazd, Iran. [6]Asma Talebian and Motahareh Soltani contributed equally to this work. ✉email: s_karami@kmu.ac.ir; somayyehkarami@gmail.com; Mehdi.Ranjbar@kmu.ac.ir

iron that are octahedrally coordinated with tetrahedral silica layers[14]. Bentonite, a cationic clay (depicted in Fig. 1b), exhibits a nearly constant negative surface charge[15]. The charge distribution, internal surface area, and heat resistance of bentonite may make it a suitable adsorbent for cationic herbicides[16,17]. The high adsorption capacities of bentonite for organic pollutants can be attributed to its swelling characteristics, internal and external cationic exchange capacity, and the availability of its interlamellar region for adsorption[18–20]. Several strategies have been used to enhance the adsorption capacity of bentonite nanostructures, including bentonite/CTAB[21], bentonite/$Mg(OH)_2$[22], bentonite/γ-alumina[23], graphene oxide/bentonite[24], and graphene oxide/bentonite-supported nano-iron[25]. Modification with nonylammonium chloride has increased bentonite interlayer spacing and PQ adsorption capacity through the exchangeability of ammonium cation with the clay interlayer cation[26]. A study confirmed that bentonite-supported zero-valent iron nanostructures were effective in PQ adsorption[20,27]. Bentonite-supported mesoporous silica nanostructures showed better PQ adsorption compared to bentonite due to electrostatic interactions[28].

Boron, identified as a metalloid element, has been demonstrated to impact a range of biological factors in animals, such as electrolyte levels, hormonal concentrations, antioxidant defense systems, and the lipid profile of the blood[29–31]. In medicine, boron compounds are used for treating arthritis, osteoporosis, and coronary heart disease[29,32]. Boron, a metalloid element, has been shown to influence various biological parameters in animals, including electrolyte levels, hormone concentrations, antioxidant defense systems, and blood lipid profiles[33,34]. As depicted in Fig. 1c, BA is classified as a weak Lewis acid due to its ability to accept a pair of nonbonding electrons. BA exhibits a trigonal-planar geometry as a consequence of the distribution of electrons in the valence shell of the boron atom, with electrons occupying only three locations. This arrangement results in sp^2 hybridization of the boron atom, creating an unoccupied $2p_z$ orbital. Consequently, BA can function as an electron-pair acceptor or Lewis acid by utilizing the vacant $2p_z$ orbital to attract a pair of nonbonding electrons from a Lewis base, thereby forming a covalent bond[35,36]. One of the most significant uses of boric acid (BA) is in neutron capture therapy for various types of cancers[37]. The bipyridyl groups in paraquat (PQ) (Fig. 1a) confer nucleophilic characteristics, enabling it to act as a Lewis base by donating a pair of nonbonding electrons[38]. It is expected that boric acid-functionalized bentonite nanostructures (BABTs) will likely show a specific binding affinity towards PQ due to the unique properties of bentonite and boric acid. To the best of our knowledge, this study is the first to explore the synergistic therapeutic potential of BABTs in mitigating PQ-induced pulmonary fibrosis. Unlike previous studies that investigated bentonite's adsorption of organic pollutants, such as paraquat[20,28], or BA's antioxidant effects in other models (e.g., bleomycin-induced fibrosis[39] or cisplatin-induced nephrotoxicity[40]), our work uniquely combines BA's Lewis acid properties with bentonite's electrostatic adsorption capacity to target PQ's nucleophilic characteristics, thereby reducing its bioavailability and associated lung damage. In this study, BABTs were synthesized and characterized using SEM, DLS, UV, and FT-IR analyses. Their binding affinity to PQ and their antioxidant, anti-inflammatory, and anti-fibrotic effects on PQ-induced histopathological injuries and lipid peroxidation in rat lung tissues were evaluated. These findings position BABTs as a promising therapeutic candidate for managing herbicide-related lung toxicities, addressing a critical gap in current treatment options.

Materials and methods

Chemicals

All chemicals were of analytical grade unless otherwise specified. Bentonite (sodium montmorillonite, ≥ 98% purity) was obtained from Dr. Mojallali Industrial Chemical Complex Co. (Arak, Iran). Boric acid (≥ 99.5% purity, catalog no. 100165) and paraquat dichloride (42% purity) were sourced from Kavosh Kimia Co. Ltd. (Iran). Other reagents, including those used for biochemical assays (e.g., malondialdehyde, superoxide dismutase, glutathione, and catalase kits) and histological staining (e.g., hematoxylin and eosin, Masson's Trichrome), were purchased from Sigma-Aldrich Chemical Co. (St. Louis, MO, USA). Deionized water was used throughout the experiments to ensure consistency in nanoparticle synthesis and biochemical analyses.

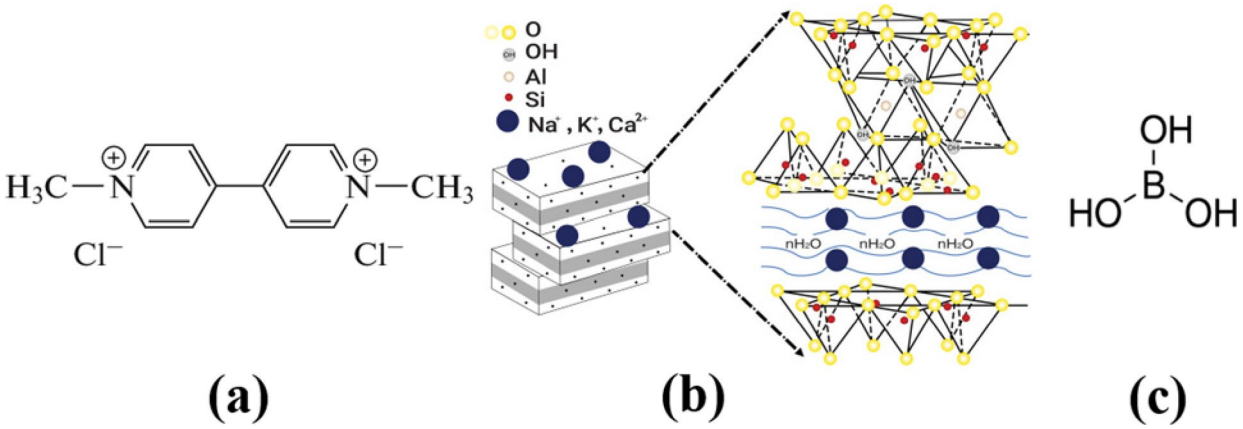


Fig. 1. Structure of (**a**) Paraquat, (**b**) Bentonite, and (**c**) Boric acid.

Instruments

A scanning electron microscope (SEM) was used to analyze the surface morphology of bentonite nanostructures. The mean size and size distribution of BABTs were determined using dynamic light scattering with a Malvern Nano ZS light scattering apparatus (Worcestershire, Malvern Instruments Ltd., UK). Ultraviolet spectroscopy (UV) spectra were obtained using the GBC CINTRA 20 instrument within the wavelength range of 200–400 nm. All nanostructures were recorded by Fourier-transform infrared (FT-IR) spectra (Shimadzu IRPRESTIGE-21 IR spectrophotometer) over the range of 400–4000 cm^{-1} using the KBr disc method.

Preparation of BABTs

To prepare BABTs (Fig. 2), bentonite powder (10 mg) was dispersed in a mixture of ethanol (2 mL) and deionized water (8 mL) in three Erlenmeyer flasks and heated at 40 °C for 30 min with continuous stirring using a magnetic stirrer. Subsequently, the surfactant cetyl trimethyl ammonium bromide (10 mg) was added to the above solutions, and they were placed in a reflux system for 30 min. Following this, the solutions were subjected to microwave radiation (300 W) for 5 min to produce nanometer-sized bentonite (characterized by DLS analysis). In the second step, boric acid (BA) powder (10, 50, or 100 mg) was added to each of the three Erlenmeyer flasks, which were then placed in a reflux system for 45 min. To co-phase bentonite and boric acid, all three solutions were exposed to microwave radiation (300 W) for 5 min to produce nanometer-sized BABTs. Finally, the as-prepared BABTs were characterized using SEM, UV, and FT-IR.

Animals

Male Wistar rats, 8 weeks old and each weighing 200 ± 25 g, were obtained from the animal house and research center of Kerman University of Medical Sciences, Kerman, Iran. The rats were kept under controlled conditions of temperature (25 ± 2 °C) and humidity (50 ± 5%) with a 12:12-h light/dark cycle in specific cages for 1 week before use. They were provided with standard rat chow and drinking water ad libitum.

This study was approved by the Ethical Committee of Kerman University of Medical Sciences, Kerman, Iran (Ethic approval code: IR.KMU.REC.1400.362). All experimental procedures were conducted in accordance with the relevant guidelines and regulations, including the National Institutes of Health Guide for the Care and Use of Laboratory Animals. This study is reported in accordance with the ARRIVE guidelines (https://arriveguidelines.org) for the reporting of animal experiments.

Pilot study

To determine an effective dose for inducing pulmonary fibrosis without mortality, a pilot study was conducted where rats were orally administered a single dose of paraquat (PQ) at 50 or 100 mg/kg. After 14 days, lung tissues were examined for histological changes via hematoxylin and eosin (H&E) staining and for fibrosis severity via Masson's trichrome staining. The severity of histological changes was classified as none (−), mild (+), moderate (++), or severe (+++)[41]. The extent of fibrosis was assessed based on the Ashcroft criteria[42]. The pilot study results demonstrated that a single oral dose of 100 mg/kg PQ induced significant pulmonary fibrosis within 14 days without causing mortality, consistent with previous studies reporting that this dose effectively induces lung injury and fibrosis in rat models without fatalities[1,43,44]. Consequently, the 100 mg/kg single oral dose of PQ was selected for further investigation in this study.

Experimental design

To investigate whether synthesized BABTs modulated PQ-induced pulmonary injuries, 48 male Wistar rats were randomly assigned to eight experimental groups, with six rats in each group. All groups except Group I received a single oral dose of 100 mg/kg aqueous solution of PQ by gastric gavage on the first day. Thirty

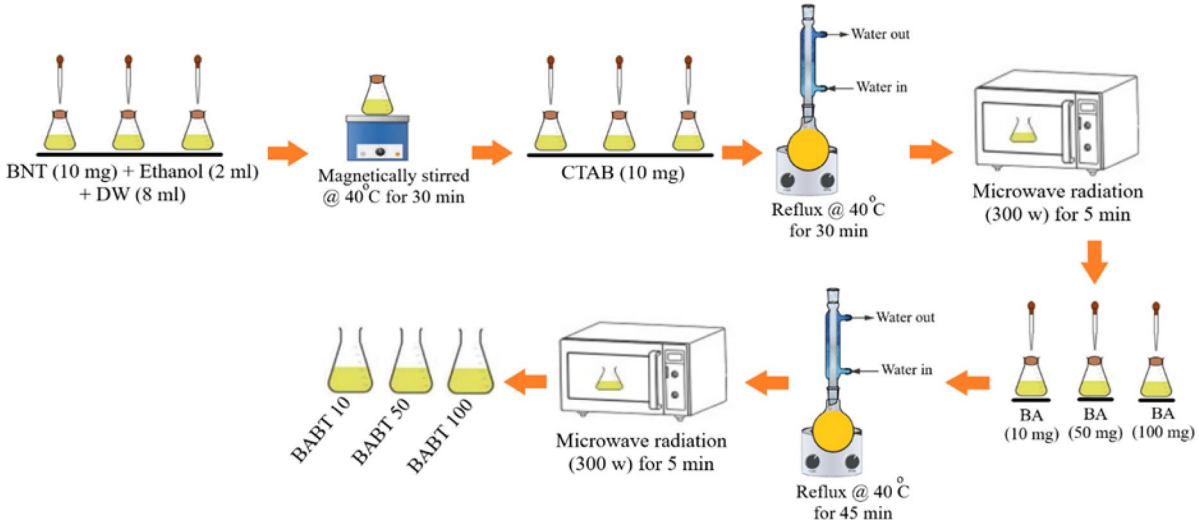


Fig. 2. Preparation of BABT nanostructures.

minutes after PQ administration, the respective treatments (BABTs or BA at 10, 50, and 100 mg/kg/day) were initiated and continued once daily for 14 consecutive days to establish a therapeutic intervention model rather than a preventive protocol. Group I, the negative control group, received 1 ml of 0.9% NaCl solution orally for 14 days. Group II, the positive control group, received a single oral dose of 100 mg/kg of PQ. Groups III, IV, and V were PQ-poisoned rats that received BABTs containing 10, 50, and 100 mg of BA/kg/day orally (PQ + BABT10, PQ + BABT50, and PQ + BABT100). Groups VI, VII, and VIII were PQ-poisoned rats that received 10, 50, and 100 mg/kg/day of BA orally (PQ + BA10, PQ + BA50, and PQ + BA100).

Tissue collection and analytical procedures

The rats were sacrificed 14 days after PQ treatment, and the lung tissues were collected to evaluate lipid peroxidation and pathological alterations. Briefly, the rats were deeply anesthetized by intraperitoneal injection of Ketamine (90 mg/kg) and Xylazine (10 mg/kg). While under deep anesthesia, the animals were euthanized by thoracotomy, and the lungs were immediately removed and washed with saline. All procedures were carried out in accordance with the ARRIVE guidelines and the AVMA Guidelines for the Euthanasia of Animals.The left lung lobe was separated and stored in 10% neutral buffered formalin for histopathological evaluation. The right lobe was used to prepare a tissue homogenate in a potassium phosphate buffer, pH 7.4. The obtained homogenates were immediately frozen at − 80 °C for lipid peroxidation evaluation.

Lipid peroxidation assay

Lipid peroxidation is commonly assessed by quantifying the malondialdehyde (MDA)[45] levels in tissues, serving as a marker for lipid peroxidation, using thiobarbituric acid (TBA). The tissue samples were homogenized with 20% trichloroacetic acid and centrifuged at 4000 rpm for 10 min, and then the precipitate was reconstituted in 0.05 mM H2SO4. Subsequently, TBA solution (0.2% in sodium sulfate) was added to the mixture and incubated in a boiling water bath for 30 min. The resulting lipid peroxidation adducts were extracted using n-butanol, and the absorbance was measured at 532 nm. The extent of lipid peroxidation was expressed as mmol MDA/mg protein of tissue according to a MDA standard curve[46].

Histopathological examination

The lung specimens were fixed in a 10% formalin solution and embedded in paraffin. The tissue sections, 5 µm thick, of the fixed lung tissues were prepared. For each animal, five tissue sections were analyzed. The sections were stained using hematoxylin and eosin (H & E) as well as Masson's Trichrome staining methods. The method proposed by Szapiel et al.[47] was employed to assess the degree of alveolitis. A total of 10 random fields/slides were examined. The average score of all the fields in each section was considered the alveolitis score. The extent of fibrosis was graded according to the Ashcroft criteria[42]. Similar to the alveolitis score, a total of 10 random fields/slides were analyzed. The average score of all the fields in each section was considered the fibrosis score. All histopathological evaluations, including H&E and Masson's Trichrome staining, were performed by an experienced pathologist who was blinded to the group assignments to ensure unbiased assessment of alveolitis and fibrosis scores.

Statistical analysis

The results were expressed as the mean ± standard deviation (SD). The statistical analyses were carried out by one-way analysis of variance (ANOVA) followed by Tukey's post hoc test using GraphPad Prism version 6 (GraphPad Software Inc., San Diego, CA, USA). The data were analyzed using SPSS version 20. The differences with a p-value less than 0.05 were considered significant in all cases. The histopathological data compared between groups underwent the Kruskal–Wallis multiple comparison test, and the Mann–Whitney U test was conducted for binary comparisons.

Results

Characterization of BABTs and evaluation of their bonding to PQ

Scanning electron microscopy (SEM) analysis revealed that boric acid-functionalized bentonite nanostructures (BABTs) possess a layered and porous morphology. The dimensions of these nanostructures ranged from approximately 34 to 136 nm. The images in Fig. 3a, b illustrate the SEM micrographs of BABTs at magnifications of 1 µm and 500 nm, respectively.

Based on the DLS analysis, the average dimensions of BABTs ranged from approximately 20–60 nm. Statistical parameters related to the distribution of BABTs were determined, with values for the distribution number (Dn) at different percentiles as follows: Dn 10%: 28.17 nm, Dn 50%: 35.5 nm, and Dn 90%: 56.36 nm. Figure 4 illustrates the DLS analysis of the BABTs.

The ultraviolet (UV) absorption spectra of the synthesized BABTs, paraquat (PQ), and the PQ-BABT complex are illustrated in Fig. 5. The peak absorption intensity of PQ and PQ-BABTs complex is consistent at 260 nm without any shift in position. However, there is a notable reduction in the absorption peak intensity of the PQ-BABTs complex at 260 nm compared to that of PQ. These findings suggest that upon exposure to UV light, the active sites of BABTs become inactive as a result of bonding with PQ molecules. Consequently, in the PQ-BABTs complex, the presence of PQ molecules occupying the active sites of BABTs leads to a decrease in electron excitation and absorption peak intensity.Ù

Fourier-transform infrared (FT-IR) spectroscopy involves acquiring an interferogram of a sample signal using an interferometer, followed by applying a Fourier transform for data analysis[42]. The FT-IR spectrum (Fig. 6a) exhibits band characteristics of the PQ molecule centered at 3052 and 3107 cm^{-1}, which are assigned to the C–H stretching mode of the methyl groups on the aromatic ring in the PQ molecule[48]. A characteristic set of bands can also be seen between 1200 and 1600 cm^{-1}, which may be assigned to the C–C stretching mode and the C-H

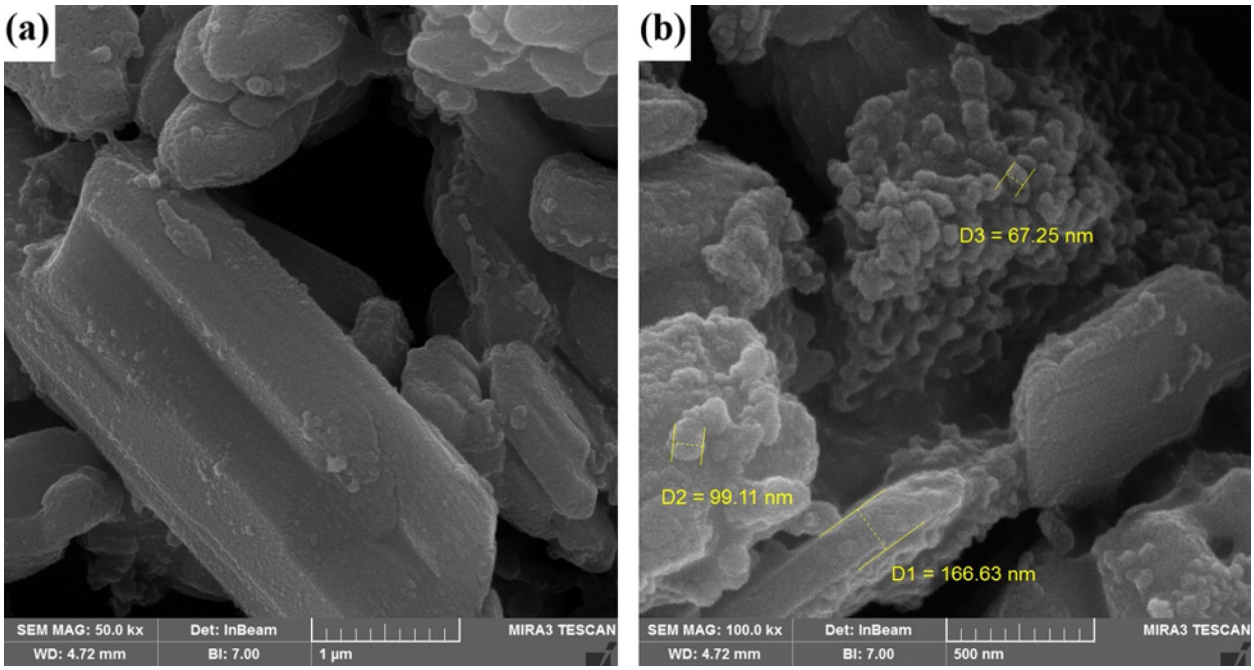


Fig. 3. SEM images of the Bentonite nanostructures at scale 1 µm (**a**), and scale 500 nm (**b**).

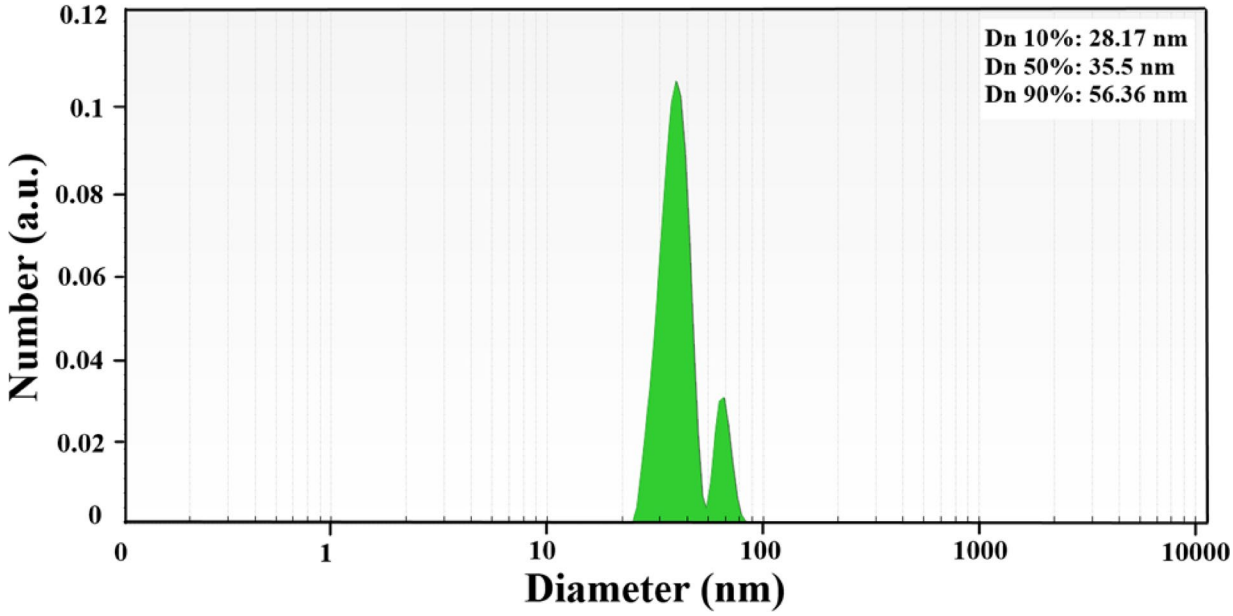


Fig. 4. DLS analysis of Boric acid-functionalized Bentonite nanostructures (BABT).

deformation mode in the aromatic ring plane[48,49]. Furthermore, the band at 1640 cm^{-1} is related to the stretching vibration of C=N/C–N in the PQ structure[50]. In Fig. 6b, the FT-IR spectra of the produced BABTs are shown within the 400–4000 cm^{-1} range. The spectrum of the BABTs exhibits a broad peak at 3453 cm^{-1}, associated with the stretching vibrations of OH functional groups from crystallization water molecules. Another peak at 1637 cm^{-1} is linked to OH deformation caused by the existence of water between bentonite layers. Furthermore, a peak at 1046 cm^{-1} is attributed to the asymmetric stretching vibrations of Si–O–Si[51,52]. The band at 1420 cm^{-1} is related to the B–O asymmetric stretching of trigonal B and B–OH in-plane bending of trigonal B[53].

Mechanism of PQ adsorbed onto BABTs

The mechanism of PQ adsorption was investigated using FT-IR before and after adsorption (Fig. 7). The FT-IR spectra of the prepared BABTs showed four principal peaks corresponding to –OH functional groups (3453 cm^{-1}),

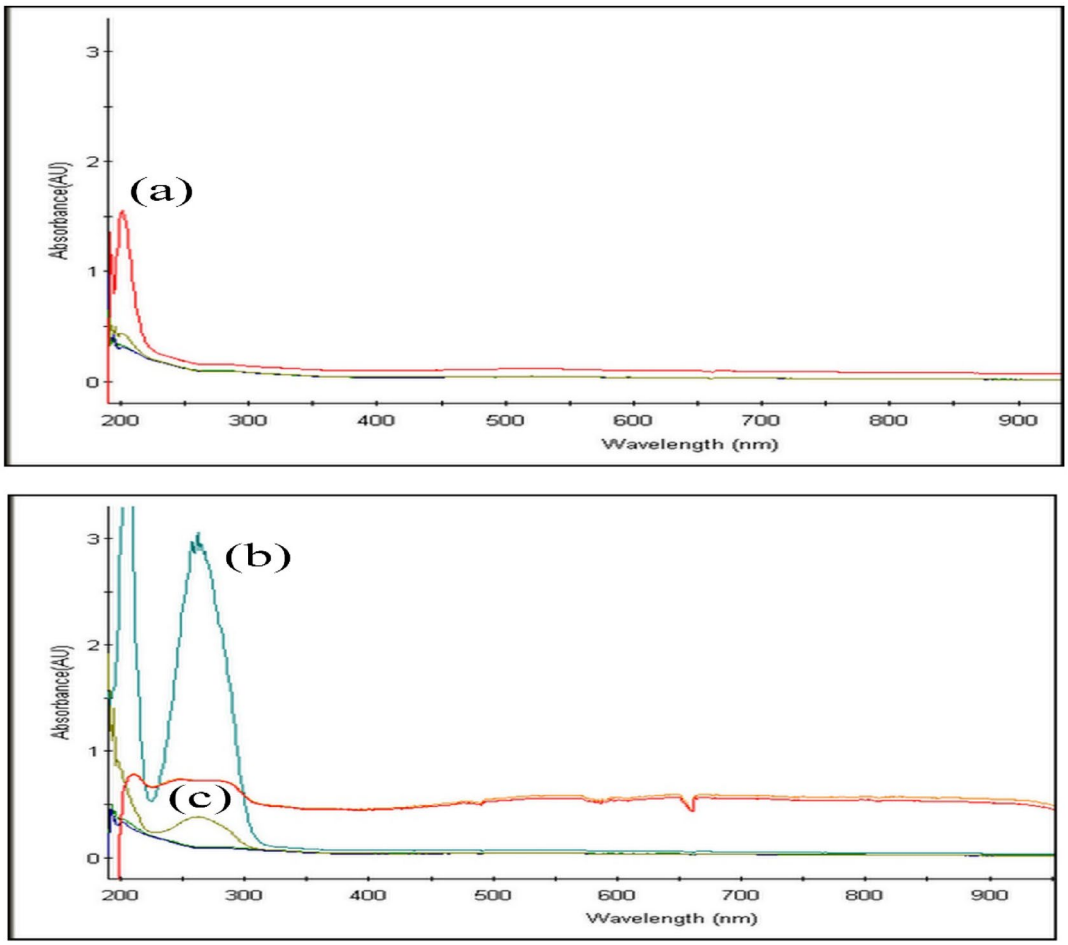


Fig. 5. UV absorption spectra of (**a**) Boric acid-functionalized Bentonite nanostructures (BABT), (**b**) Paraquat (PQ), and (**c**) PQ-BABT complex. The star symbol indicates the absorption peak of PQ occurs at 260 nm.

–OH deformation (1637 cm^{-1}), Si–O–Si bonds (1046 cm^{-1}), and B–O and B–OH bonds (1420 cm^{-1}). However, the FT-IR spectra after PQ adsorption showed shifted peaks. The shifts attributed to -OH, -OH deformation, Si–O–Si, and B–O and B–OH, shifted by – 3 cm^{-1}, – 2 cm^{-1}, – 2 cm^{-1}, and – 3 cm^{-1}, respectively, confirming the interaction between these groups and PQ.

Effect of BABTs on lipid peroxidation

The levels of MDA in the samples were assessed as a measure of lipid peroxidation. The research findings demonstrated a notable rise in MDA levels in the rats treated with PQ ($P < 0.0001$) compared to those in the control group. Figure 8 shows a significant reduction in MDA levels in the rats treated with both PQ and BABT50 compared to those treated solely with PQ ($P < 0.05$). No significant differences in MDA concentration were observed between the remaining experimental groups and the PQ-treated rats. The results depicted in Fig. 8 indicated a significant increase in MDA levels in the PQ + BABT10, PQ + BABT100, and PQ + BA50 groups ($P < 0.05$) as well as the PQ + BA100 group ($P < 0.001$) when compared to those in the control group.

Effect of BABTs on histopathological alterations

Evaluation of the H&E-stained and Masson's Trichrome-stained sections revealed that the normal lung architecture was destroyed following PQ administration, and a fibrotic pattern was observed. The tissue photomicrographs in the control group displayed ideal lung architecture. In the PQ group, extensive tissue damage was evident, with destroyed alveoli, thickening of the alveolar wall, accumulation of inflammatory cells, atelectasis, and lung fibrosis. The tissue images of the PQ group treated with BABTs showed significant recovery with a considerable decrease in the fibrosis score. No observable differences in pathological changes were noted between the BABT-treated groups. No significant restoration was observed in the PQ group treated with BA, with the tissue structure remaining similar to that of the PQ group, showing alveolar destruction, atelectasis, accumulation of inflammatory cells, and thickening of the alveolar walls (Table 1).

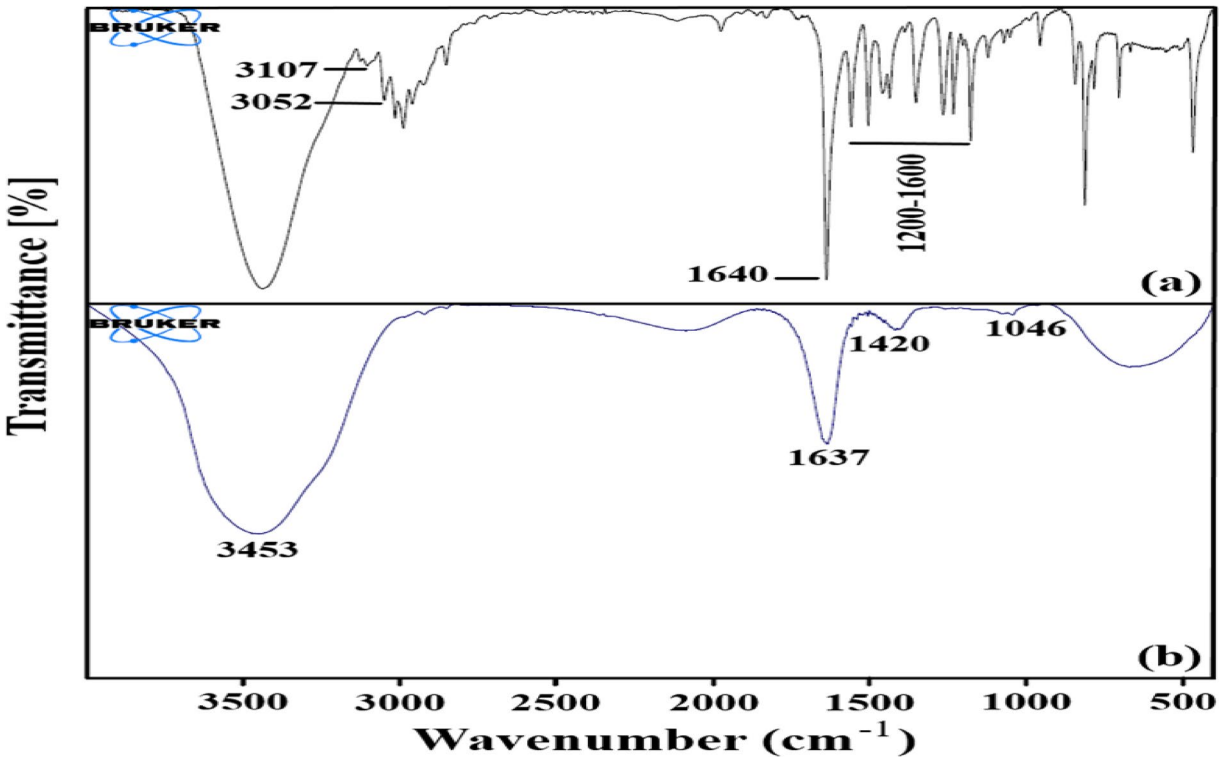


Fig. 6. FT-IR spectra of (**a**) Paraquat (PQ), and (**b**) Boric acid-functionalized Bentonite nanostructures (BABT).

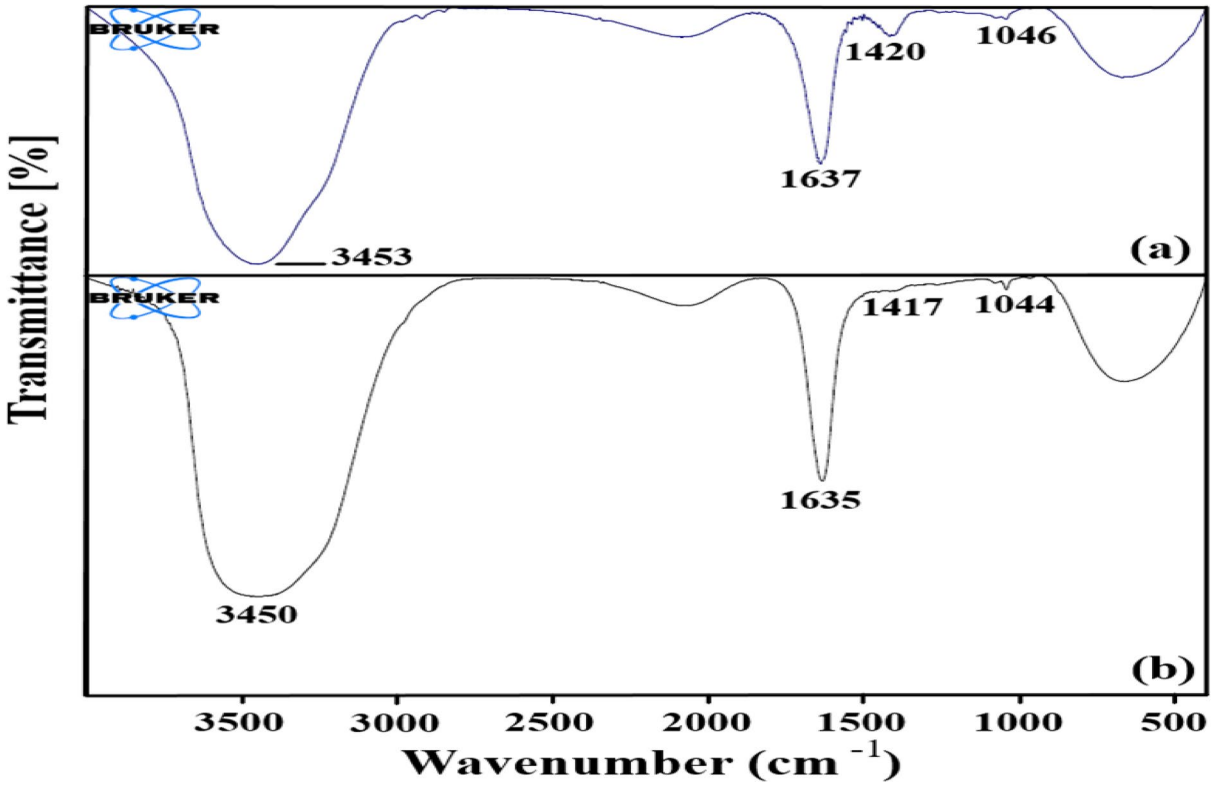


Fig. 7. FT-IR spectra of (**a**) Boric acid-functionalized bentonite nanostructures (BABT), and (**b**) PQ-BABT complex.

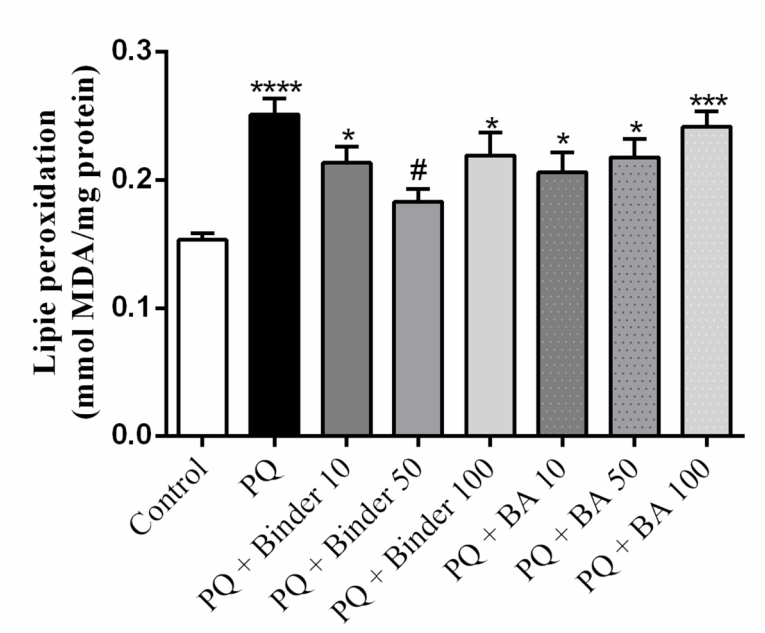


Fig. 8. Effect of treatment with Boric acid-functionalized Bentonite nanostructures (BABT) on the levels of malondialdehyde (MDA) in lung tissue homogenate in PQ-induced oxidative stress. Values are expressed as Mean ± SD (n = 6). * Significant increase in comparison with the Control group ($^{*}P < 0.05$, $^{***}P < 0.001$, $^{****}P < 0.0001$). #Significant decrease in comparison with the Paraquat (PQ) group ($^{\#}P < 0.05$).

Animal group	Emphysema	Atelectasis	Inflammation	Alveolar hemorrhage	Fibrosis score
Control	–	–	–	–	2
50 mg/kg PQ	+	+ +	+	–	5
100 mg/kg PQ	+	+ + +	+ +	+	8

Table 1. Lung histopathology results after oral administration of Paraquat (PQ) in a pilot study.

Determination of inflammation in the histopathologic study by Szapiel scoring method

The Szapiel score of the PQ group exhibited a statistically significant increase compared to that of the normal control group ($P < 0.0001$). In contrast, the Szapiel scores of the BABT10 and BABT50 treated groups showed a significant decrease ($P < 0.05$), while the BABT100 treated group displayed an even more pronounced reduction ($P < 0.001$) compared to the PQ group. These findings indicated the anti-inflammatory properties of BABTs. Conversely, the BA-treated groups did not demonstrate a notable decrease in Szapiel scores, suggesting that BA did not yield a significant anti-inflammatory effect on PQ-intoxicated rats (refer to Fig. 9 and Table 2).

Assessment of lung fibrosis degree by Ashcroft scoring method in the histopathologic study

The histopathological examination showed that exposure to PQ caused tissue damage and fibrotic changes, as indicated by a significant difference ($P < 0.001$). After administering BABTs orally in the PQ-induced lung injury model, a statistically significant decrease in the extent of fibrosis was observed ($P < 0.05$). In contrast, treatment with BA did not result in a significant reduction in the observed damage. As a result, the groups treated with BABTs showed a marked decrease in the severity of fibrosis compared to that in the PQ-exposed group, as depicted in Fig. 10 and Table 2.

Discussion

This study evaluated the antioxidant, anti-inflammatory, and anti-fibrotic effects of boric acid-functionalized bentonite nanostructures (BABTs) on paraquat (PQ)-induced lung injuries. The findings from examinations utilizing DLS and SEM demonstrated that BABTs exhibited dimensions ranging from 20 to 60 nm and displayed the intended morphology. FT-IR and UV spectroscopy confirmed active components on BABTs' surface, validating their interaction with paraquat to form the PQ-BABTs complex. Notably, when compared to BA, the administration of BABTs at a dose of 50 mg/kg led to a substantial reduction in the lung lipid peroxidation levels and demonstrated significant improvement in histological outcomes.

Oxidative stress, inflammation, and fibrosis were identified as key factors in the development of these injuries following exposure to PQ. Exposure to PQ can result in significant and irreversible lung injury, leading to fibrosis

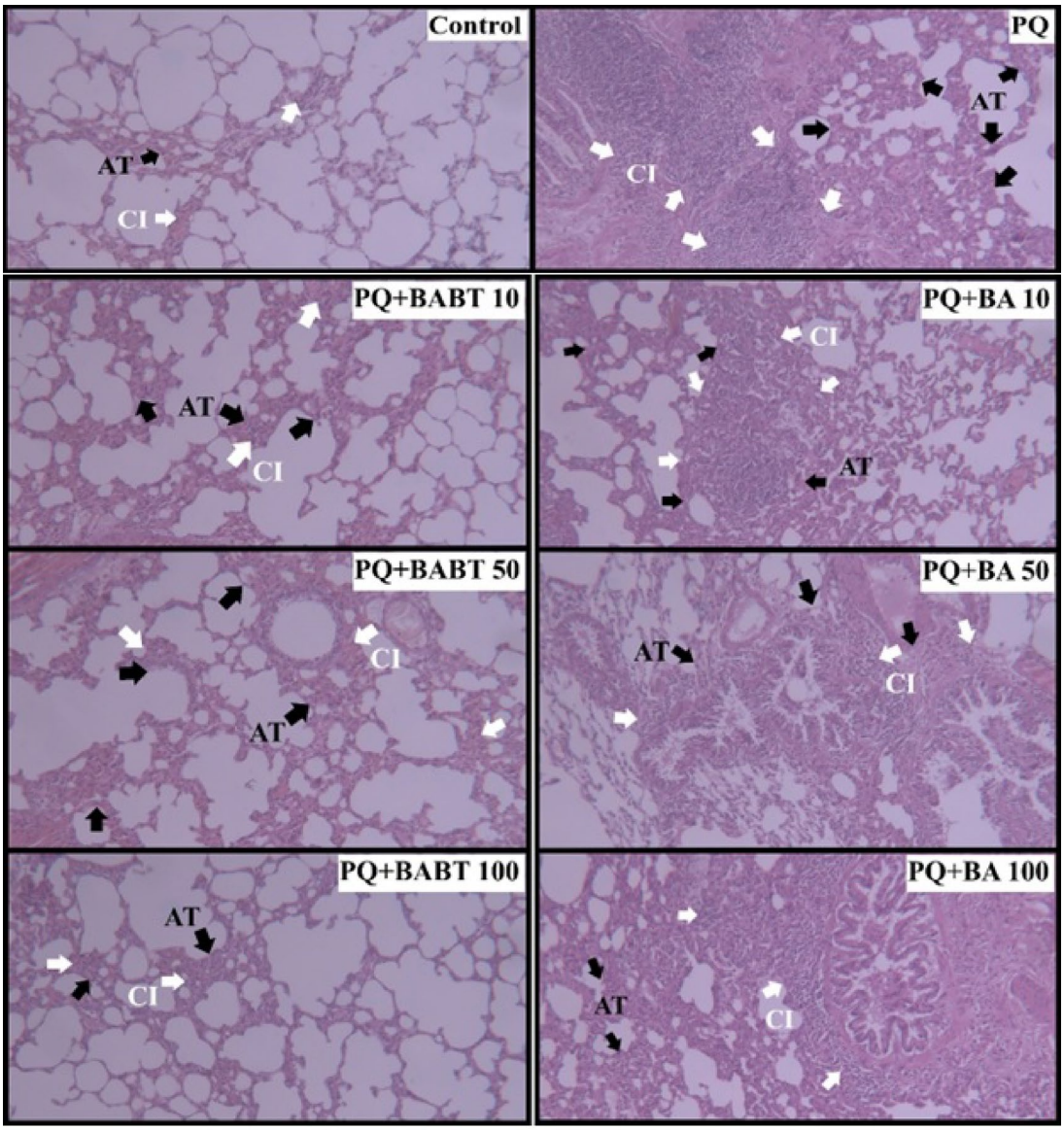


Fig. 9. H&E-stained histological evaluation of rat lungs in the Control, Paraquat (PQ), Paraquat with Boric acid-functionalized Bentonite nanostructures (PQ + BABT), and Paraquat with Boric acid (PQ + BA) groups on day 14 after PQ administration (× 100 magnification, Scale bar= 200 μm). Compared with the Control group, PQ intoxication showed progressive atelectasis and accumulation of inflammatory cells (chronic inflammation) in the alveolar space and septum. BABT nanostructures-treated groups showed remarkably decreased atelectasis (AT) and chronic inflammation (CI), while these changes were no less in the BA-treated groups.

that shares similarities with the toxic effects observed in other pulmonary agents, such as bleomycin[54]. In cases of PQ toxicity, oxidative stress in pulmonary cells, particularly alveolar type I and type II epithelial cells, is caused by the generation of free radicals and reduction of antioxidants, which consequently results in cellular and tissue oxidative damage through the development of macromolecular oxidation, including lipid peroxidation, and protein carbonylation[55]. Enzymatic and non-enzymatic antioxidant enzyme systems protect the lungs from oxidative damage. Exposure to toxic substances can affect the function of antioxidant enzymes and decrease the levels of antioxidants such as glutathione[56–58]. Following oxidative injury, pulmonary cell death triggers alveolitis and pulmonary edema, ultimately leading to marked lung fibrosis during the proliferative stage[43]. The results of this study demonstrated the significant fibrogenic effect of PQ on lung tissues, accompanied by elevated levels of lipid peroxidation as an oxidative stress marker in the PQ-treated group, potentially by enhancing the activity of antioxidant enzymes in the injured lung tissue.

Our findings showed that BABTs significantly attenuated PQ-induced fibrosis in rat lungs. Bentonite, as an adsorbent with molecular sieving properties, reduced lipid peroxidation and mitigated oxidative stress[59]. BA also exhibits strong antioxidant properties by efficiently scavenging free radicals and superoxide radicals. It also supports the function of different antioxidant enzymes and reduces the concentrations of inflammatory

Animal group	Fibrosis score (The Ashcroft scale)	Alveolitis score (The Szapiel scale)
Control	2.1 ± 0.57	1.6 ± 0.54
PQ	8 ± 1***	3.4 ± 0.54****
PQ + BABT 10	5.5 ± 0.57*	2.2 ± 0.44*
PQ + BABT 50	5.5 ± 0.57*	2.2 ± 0.44*
PQ + BABT 100	5.25 ± 0.5*	1.8 ± 0.44***
PQ + BA 10	7.25 ± 0.5**	2.6 ± 0.54
PQ + BA 50	7.25 ± 0.5**	2.8 ± 0.44*
PQ + BA 100	7.25 ± 0.5**	2.8 ± 0.44*

Table 2. Comparisons of alveolitis score and fibrosis score among groups of control, Paraquat (PQ) treatment, Paraquat with boric acid-functionalized bentonite nanostructures (PQ + BABT) treatment, and Paraquat with boric acid (PQ + BA) treatment (Mean ± SD; n = 6). Data were analyzed by the Kruskal–Wallis multiple comparison test followed by the Mann–Whitney U post hoc test for multiple comparisons. * Significant increase in comparison with the Control group ($^{*}P < 0.05$, $^{**}P < 0.01$, $^{***}P < 0.001$, $^{****}P < 0.0001$). * Significant decrease in comparison with the Paraquat (PQ) group ($^{*}P < 0.05$, $^{***}P < 0.001$).

biomarkers[60]. Following our results, Sogut et al. illustrated the hepatoprotective benefits of BA in rats subjected to chronic alcohol consumption by its antioxidative and antiapoptotic characteristics[61]. Previous studies have reported BA's ability to ameliorate pulmonary fibrosis triggered by bleomycin and renal impairment induced by cyclophosphamide[39,62]. These observations are consistent with earlier investigations suggesting that BA could alleviate cisplatin-induced nephrotoxicity by mechanisms such as the inhibition of oxidative stress, inflammation, and apoptotic damage in the serum, red blood cells, and kidney tissues of rats[40]. Previous studies also found the protective effect of BA against lung toxicity induced by other agents, such as bleomycin and formaldehyde[39,63]. As expected, the lipid peroxidation results aligned with the histopathology findings in the lung tissue. The findings from the tissue staining using Masson's Trichrome support previous studies indicating that PQ induces the accumulation of collagen and the development of lung fibrotic lesions[54,64]. The BABTs were found to significantly reduce collagen deposition and pulmonary fibrosis in histopathology findings.

The present study demonstrates that BABTs mitigate PQ-induced pulmonary damage. In addition to the attenuating effect of BABTs on pulmonary injury and fibrosis through their potent antioxidant properties, the noted protective effect could be attributed to other various factors. Firstly, it could be due to the bonding of PQ molecules with BABTs. The adsorption mechanism of PQ onto BABTs involves a Lewis acid–base interaction between BA and PQ molecules, facilitated by dative bonds, resulting in the generation of additional products[60]. Secondly, the protective effect may also be influenced by the electrostatic interactions between the PQ^{2+} molecules and the negative surface charge on the bentonite nanostructures. Lastly, hydrogen bonding between the OH-groups located on the surface of BABTs and the nitrogen atoms within the structure of the PQ molecule could also contribute to this protective effect.

The translational relevance of our findings lies in the potential application of BABTs for managing PQ-induced pulmonary fibrosis in humans, where rat models have been shown to closely mimic the oxidative stress, inflammation, and fibrotic progression observed in clinical cases of PQ poisoning[65]. Using FDA-recommended allometric scaling for dose extrapolation (HED = rat dose × [rat Km / human Km], where Km rat = 6 and Km human = 37, yielding a conversion factor of approximately 0.162)[66], the effective rat dose of BABTs at 50 mg/kg/day corresponds to a human equivalent dose (HED) of approximately 8.1 mg/kg/day, which could serve as a starting point for future preclinical safety studies. However, safety concerns associated with nanoparticles must be addressed; boric acid, while generally low in acute toxicity, has been linked to reproductive and developmental effects in chronic exposures[67], and bentonite NPs may pose risks of inhalation-induced lung inflammation or oxidative stress, as evidenced by increased malondialdehyde levels in exposed models[68]. General nanoparticle risks, including enhanced systemic absorption and potential organ toxicity, further necessitate rigorous toxicokinetic evaluations in larger animal models or human cell lines. Clinically, BABTs could offer a practical adjunct therapy for PQ intoxication, where current management relies on supportive measures like activated charcoal and immunosuppression without a specific antidote; by reducing PQ bioavailability through complex formation, BABTs may mitigate acute lung injury and fibrosis, potentially improving survival rates in emergency settings. Nonetheless, these implications require validation through Phase I/II clinical trials to confirm efficacy, dosing, and safety in humans. This study utilized only male Wistar rats to minimize potential confounding effects of female hormonal fluctuations, particularly estrogen, which can modulate oxidative stress and inflammatory pathways relevant to paraquat (PQ)-induced pulmonary fibrosis[69]. In initial animal studies, selecting a single sex, typically males, is a common practice to reduce variability due to hormonal influences, ensuring clearer interpretation of treatment effects[70]. Current evidence suggests that PQ toxicity mechanisms are largely consistent across genders in rat models[43]. However, female hormones may subtly influence the severity of lung injury or response to BABTs. Future studies incorporating both male and female rats are essential to confirm the generalizability of BABTs' antioxidant, anti-inflammatory, and anti-fibrotic effects across genders.

Conclusion

Collectively, BABTs exhibited a protective effect against PQ-induced pulmonary injuries across various stages of toxicity, mediated by their antioxidant, anti-inflammatory, and anti-fibrotic properties, as well as potential

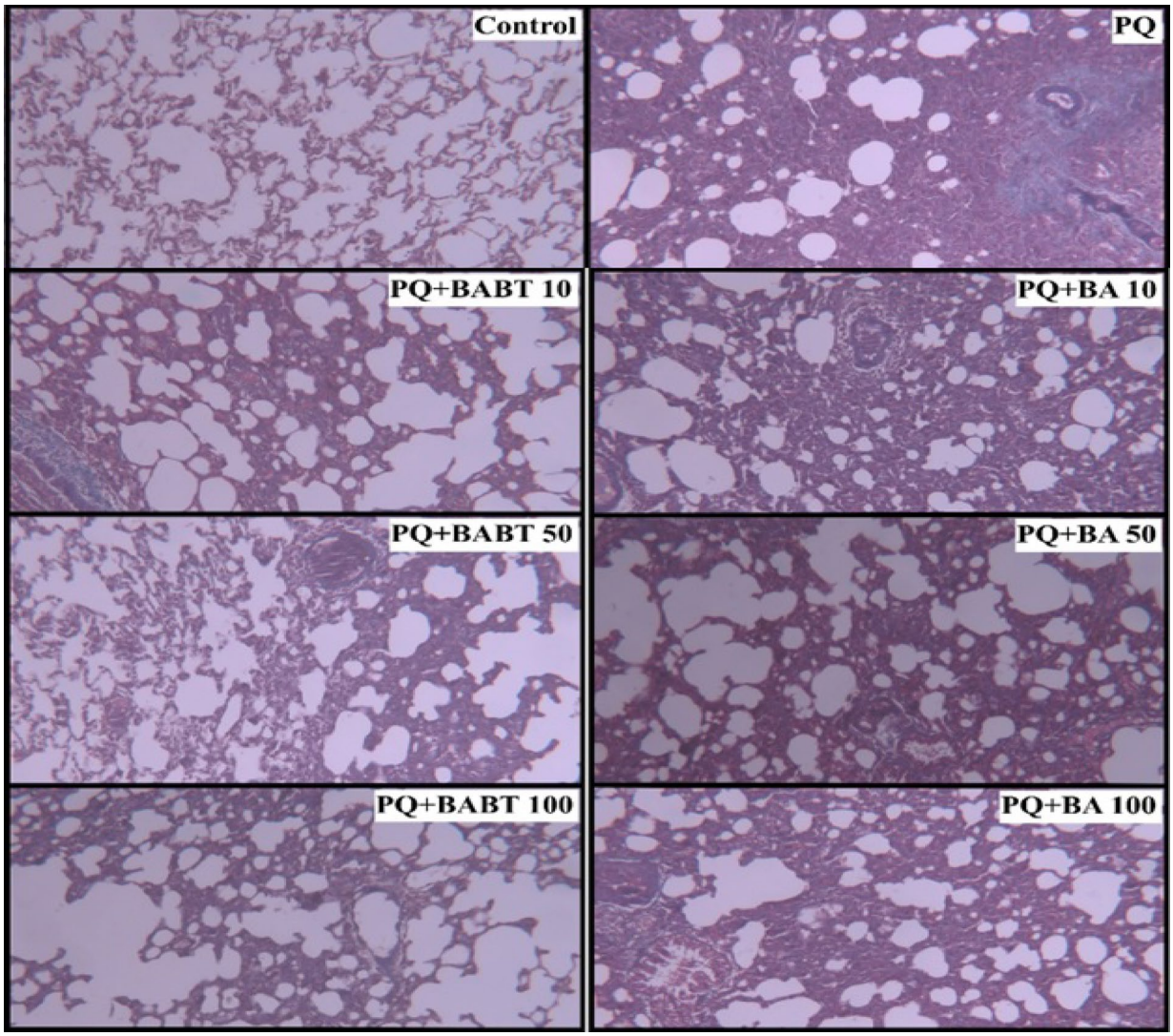


Fig. 10. Histological evaluation of rat lungs in the Control, Paraquat (PQ), Paraquat with Boric acid-functionalized Bentonite nanostructures (PQ + BABT), and Paraquat with Boric acid (PQ + BA) groups on day 14 after PQ administration with Masson trichrome stain (× 100 magnification, Scale bar= 200 µm). Compared to control, PQ exposure increased fibrosis (seen as blue collagen deposition) in the alveolar regions and small bronchioles. BABT nanostructures-treated groups exhibited decreased fibrosis scores, while these changes were no less in the BA-treated groups.

physicochemical interactions with PQ. The multifaceted antioxidant, anti-inflammatory, and anti-fibrotic activities of BABTs warrant further investigation of their therapeutic potential for pulmonary injuries induced by pharmaceuticals, toxins, or medical conditions. Future studies should incorporate direct mechanistic assays, such as reactive oxygen species (ROS) detection, NF-κB pathway inhibition, monoamine oxidase (MAO) activity measurement, and comprehensive evaluation of antioxidant defense systems (e.g., GSH, SOD, and CAT) to clarify the molecular and oxidative pathways involved in the protective effects of BABTs.

Data availability

All data generated or analyzed during this study are included in this published article.

Received: 11 September 2025; Accepted: 3 November 2025
Published online: 08 December 2025

References

1. Da Chen, T. M. et al. Rapamycin reverses paraquat-induced acute lung injury in a rat model through inhibition of NFκB activation. *Int. J. Clin. Exp. Pathol.* **8**(5), 4627 (2015).
2. Ghasemi, S. Z. et al. Paraquat-induced systemic inflammation and oxidative stress in rats improved by Curcuma longa ethanolic extract, curcumin and a PPAR agonist. *Toxicon* **227**, 107090 (2023).

3. Vale, J., Meredith, T. & Buckley, B. Paraquat poisoning: Clinical features and immediate general management. *Hum. Toxicol.* **6**(1), 41–47 (1987).
4. Baltazar, T. et al. Paraquat research: Do recent advances in limiting its toxicity make its use safer?. *Br. J. Pharmacol.* **168**(1), 44–45 (2013).
5. Rose, M. S., Smith, L. L. & Wyatt, I. Evidence for energy-dependent accumulation of paraquat into rat lung. *Nature* **252**(5481), 314–315 (1974).
6. Forman, H. et al. Differential paraquat uptake and redox kinetics of rat granular pneumocytes and alveolar macrophages. *J. Pharmacol. Exp. Ther.* **221**(2), 428–433 (1982).
7. Ranjbar, A. Evidence of oxidative damage in paraquat toxicity. *Zahedan J. Res. Med. Sci.* **16**(12), 1–8 (2014).
8. Shahabadi, N. et al. A dose-related positive effect of inhaled simvastatin-loaded PLGA nanoparticles on paraquat-induced pulmonary fibrosis in rats. *Basic Clin. Pharmacol. Toxicol.* **131**(4), 251–261 (2022).
9. Carre, P. & Leophonte, P. Cytokines and pulmonary fibroses. *Rev. Mal. Respir.* **10**(3), 193–207 (1993).
10. Melchiorri, D. et al. Paraquat toxicity and oxidative damage: Reduction by melatonin. *Biochem. Pharmacol.* **51**(8), 1095–1099 (1996).
11. Lewis, C. & Nemery, B. *Pathophysiology and biochemical mechanisms of the pulmonary toxicity of paraquat.* (1995).
12. Gil, H.-W. et al. Relationship between pulmonary surfactant protein and lipid peroxidation in lung injury due to paraquat intoxication in rats. *Korean J. Intern. Med.* **22**(2), 67 (2007).
13. Hwang, K.-Y., Lee, E.-Y. & Hong, S.-Y. Paraquat intoxication in Korea. *Arch. Environ. Health Int. J.* **57**(2), 162–166 (2002).
14. Rouquerol, F., Rouquerol, J. & Sing, K. *Assessment of surface area. Adsorption by powders and porous solids* (London: Academic Press, 1999).
15. Mockovčiaková, A., Orolínová, Z. & Škvarla, J. Enhancement of the bentonite sorption properties. *J. Hazard. Mater.* **180**(1–3), 274–281 (2010).
16. Ganigar, R. et al. Polymer–clay nanocomposites for the removal of trichlorophenol and trinitrophenol from water. *Appl. Clay Sci.* **49**(3), 311–316 (2010).
17. Paul, B. et al. Adsorption of the herbicide simazine on moderately acid-activated beidellite. *Appl. Clay Sci.* **49**(1–2), 80–83 (2010).
18. Awad, A. M. et al. Adsorption of organic pollutants by natural and modified clays: A comprehensive review. *Sep. Purif. Technol.* **228**, 115719 (2019).
19. Shaban, M. et al. Novel bentonite/zeolite-NaP composite efficiently removes methylene blue and Congo red dyes. *Environ. Chem. Lett.* **16**(1), 275–280 (2018).
20. Dehgani, Z. et al. Removal of paraquat from aqueous solutions by a bentonite modified zero-valent iron adsorbent. *New J. Chem.* **44**(31), 13368–13376 (2020).
21. Huang, Z. et al. Modified bentonite adsorption of organic pollutants of dye wastewater. *Mater. Chem. Phys.* **202**, 266–276 (2017).
22. Chinoune, K. et al. Adsorption of reactive dyes from aqueous solution by dirty bentonite. *Appl. Clay Sci.* **123**, 64–75 (2016).
23. Pourshadlou, S. et al. Adsorption system for Mg2+ removal from aqueous solutions using bentonite/γ-alumina nanocomposite. *J. Colloid Interface Sci.* **568**, 245–254 (2020).
24. Hongjuan, L. et al. Novel graphene oxide/bentonite composite for uranium (VI) adsorption from aqueous solution. *J. Radioanal. Nucl. Chem.* **317**(3), 1349–1360 (2018).
25. Yu, C. et al. Treatment of lead contaminated water using synthesized nano-iron supported with bentonite/graphene oxide. *Arab. J. Chem.* **13**(1), 3474–3483 (2020).
26. Seki, Y. & Yurdakoç, K. Paraquat adsorption onto clays and organoclays from aqueous solution. *J. Colloid Interface Sci.* **287**(1), 1–5 (2005).
27. Chen, Z.-X. et al. Removal of methyl orange from aqueous solution using bentonite-supported nanoscale zero-valent iron. *J. Colloid Interface Sci.* **363**(2), 601–607 (2011).
28. Rasaie, A. et al. Removal of herbicide paraquat from aqueous solutions by bentonite modified with mesoporous silica. *Mater. Chem. Phys.* **262**, 124296 (2021).
29. Khaliq, H., Juming, Z. & Ke-Mei, P. The physiological role of boron on health. *Biol. Trace Elem. Res.* **186**(1), 31–51 (2018).
30. Haseeb, K. et al. Effects of boron supplementation on expression of Hsp70 in the spleen of African ostrich. *Biol. Trace Elem. Res.* **182**(2), 317–327 (2018).
31. Ince, S. et al. Boron ameliorates arsenic-induced DNA damage, proinflammatory cytokine gene expressions, oxidant/antioxidant status, and biochemical parameters in rats. *J. Biochem. Mol. Toxicol.* **33**(2), e22252 (2019).
32. Mogoşanu, G. D. et al. Calcium fructoborate for bone and cardiovascular health. *Biol. Trace Elem. Res.* **172**(2), 277–281 (2016).
33. Türkez, H. et al. Effects of some boron compounds on peripheral human blood. *Zeitschrift für Naturforschung C* **62**(11–12), 889–896 (2007).
34. Abdelnour, S. A. et al. The vital roles of boron in animal health and production: A comprehensive review. *J. Trace Elem. Med. Biol.* **50**, 296–304 (2018).
35. Lopalco, A. et al. Boric acid, a Lewis acid with unique and unusual properties: Formulation implications. *J. Pharm. Sci.* **109**(8), 2375–2386 (2020).
36. Soltani, M. et al. Proposing boric acid as an antidote for aluminium phosphide poisoning by investigation of the chemical reaction between boric acid and phosphine. *J. Med. Hypotheses Ideas* **7**(1), 21–24 (2013).
37. Ince, S. et al. Protective effects of boron on cyclophosphamide induced lipid peroxidation and genotoxicity in rats. *Chemosphere* **108**, 197–204 (2014).
38. Kassab, E. & Castellà-Ventura, M. Theoretical study of pyridine and 4, 4 ʻ-bipyridine adsorption on the lewis acid sites of alumina surfaces based on Ab initio and density functional cluster calculations. *J. Phys. Chem. B* **109**(28), 13716–13728 (2005).
39. Çelikezen, F. Ç. et al. The antioxidant effect of boric acid and CoQ10 on pulmonary fibrosis in bleomycin induced rats. *Bitlis Eren Univ. J. Sci. Technol.* **2**(1), 27–31 (2015).
40. Hazman, Ö. et al. The effect of boric acid and borax on oxidative stress, inflammation, ER stress and apoptosis in cisplatin toxication and nephrotoxicity developing as a result of toxication. *Inflammation* **41**(3), 1032–1048 (2018).
41. Nishida, C. et al. Predictive biomarkers for the ranking of pulmonary toxicity of nanomaterials. *Nanomaterials* **10**(10), 2032 (2020).
42. Ashcroft, T., Simpson, J. M. & Timbrell, V. Simple method of estimating severity of pulmonary fibrosis on a numerical scale. *J. Clin. Pathol.* **41**(4), 467–470 (1988).
43. Dinis-Oliveira, R. et al. Paraquat poisonings: mechanisms of lung toxicity, clinical features, and treatment. *Crit. Rev. Toxicol.* **38**(1), 13–71 (2008).
44. Hübner, R.-H. et al. Standardized quantification of pulmonary fibrosis in histological samples. *Biotechniques* **44**(4), 507–517 (2008).
45. Ahmadipour, A. et al. Hepatoprotective effect of *Zataria Multiflora* Boiss against malathion-induced oxidative stress in male rats. *Orient. Pharm. Exp. Med.* **16**(4), 287–293 (2016).
46. Ohkawa, H., Ohishi, N. & Yagi, K. Assay for lipid peroxides in animal tissues by thiobarbituric acid reaction. *Anal. Biochem.* **95**(2), 351–358 (1979).
47. Szapiel, S. V. et al. Bleomycin-induced interstitial pulmonary disease in the nude, athymic mouse. *Am. Rev. Respir. Dis.* **120**(4), 893–899 (1979).

48. Haque, R. & Lilley, S. Infrared spectroscopic studies of charge transfer complexes of diquat and paraquat. *J. Agric. Food Chem.* **20**(1), 57–58 (1972).
49. Brienne, S. H. et al. Infrared spectra and theoretical studies of bridged diquaternary 2, 2′-dipyridinium compounds. *J. Mol. Struct.* **356**(2), 81–94 (1995).
50. Hsu, S.-T. & Pan, T.-C. Adsorption of paraquat using methacrylic acid-modified rice husk. *Biores. Technol.* **98**(18), 3617–3621 (2007).
51. Temuujin, J. et al. Characterisation of acid activated montmorillonite clay from Tuulant (Mongolia). *Ceram. Int.* **30**(2), 251–255 (2004).
52. Boufatit, M., Ait-Amar, H. & McWhinnie, W. Development of an Algerian material montmorillonite clay. Adsorption of phenol, 2-dichlorophenol and 2, 4, 6-trichlorophenol from aqueous solutions onto montmorillonite exchanged with transition metal complexes. *Desalination* **206**(1–3), 394–406 (2007).
53. Su, C. & Suarez, D. L. Coordination of adsorbed boron: A FTIR spectroscopic study. *Environ. Sci. Technol.* **29**(2), 302–311 (1995).
54. Dong, J. et al. Common and distinct mechanisms of induced pulmonary fibrosis by particulate and soluble chemical fibrogenic agents. *Arch. Toxicol.* **90**(2), 385–402 (2016).
55. Rashidipour, N. et al. Where ferroptosis inhibitors and paraquat detoxification mechanisms intersect, exploring possible treatment strategies. *Toxicology* **433–434**, 152407 (2020).
56. Soltani, M., et al., Reducing the cytotoxicity of magnesium oxide nanoparticles using cerium oxide shell coating: An in vitro and in vivo study *Ceram. Int.* (2023).
57. Dabaghzadeh, F., Rahimpour, M. & Karami-Mohajeri, S. Effect of vitamin D administration on blood oxidative stress factors in university students: A randomized double-blind clinical trial. *Koomesh J.* **23**(6), 712–719 (2021).
58. Soltani, M. et al. An interdisciplinary approach to assessing the toxicity reduction of cerium oxide nanoparticles coated with polyethylene glycol and polyvinylpyrrolidone polymers: An in vitro study. *Toxicology Vitro* **105**, 106022 (2025).
59. Saša, I., et al., *The application of adsorbent bentonite in oxidative stress induced by paraquat.* Acta Veterinaria (2007).
60. Naghii, M. R. et al. Comparative effects of daily and weekly boron supplementation on plasma steroid hormones and proinflammatory cytokines. *J. Trace Elem. Med Biol.* **25**(1), 54–58 (2011).
61. Sogut, I. et al. The antioxidant and antiapoptotic effect of boric acid on hepatoxicity in chronic alcohol-fed rats. *Can. J. Physiol. Pharmacol.* **96**(4), 404–411 (2018).
62. Cengiz, M. Boric acid protects against cyclophosphamide-induced oxidative stress and renal damage in rats. *Cell Mol. Biol. (Noisy-le-grand)* **64**(12), 11–14 (2018).
63. Arslan-Acaroz, D. & Bayşu-Sozbilir, N. Ameliorative effect of boric acid against formaldehyde-induced oxidative stress in A549 cell lines. *Environ. Sci. Pollut. Res.* **27**(4), 4067–4074 (2020).
64. Ghazi-Khansari, M. et al. Antifibrotic effect of captopril and enalapril on paraquat-induced lung fibrosis in rats. *J. Appl. Toxicol. Int. J.* **27**(4), 342–349 (2007).
65. Gauldie, J. & Kolb, M. Animal models of pulmonary fibrosis: how far from effective reality?. *Am. J. Physiol. Lung Cell. Mol. Physiol.* **294**(2), L151–L151 (2008).
66. FDA, U., *Guidance for industry: estimating the maximum safe starting dose in initial clinical trials for therapeutics in adult healthy volunteers.* FDA, ed, 2005.
67. Hadrup, N., Frederiksen, M. & Sharma, A. K. Toxicity of boric acid, borax and other boron containing compounds: A review. *Regul. Toxicol. Pharmacol.* **121**, 104873 (2021).
68. Blanc, P.D., et al., *26* Chronic obstructive airway disease due to occupational exposure *Asthma in the Workplace* 375 (2013).
69. Luderer, U. Ovarian toxicity from reactive oxygen species. *Vitam. Horm.* **94**, 99–127 (2014).
70. Clayton, J. A. & Collins, F. S. Policy: NIH to balance sex in cell and animal studies. *Nature* **509**(7500), 282–283 (2014).

Acknowledgements
The authors extend their sincere gratitude to the pathology laboratory of Kerman Shahid Bahonar Hospital, and particularly acknowledge the invaluable collaboration and support of its supervisors, Mrs. Donya Bafti and Mrs. Reyhaneh Hoseini. We are also deeply thankful to Mr. Ehsan Mehrabi Kermani for his diligent proofreading of the English manuscript. The authors confirm that Mr. Ehsan Mehrabi Kermani provided writing assistance by proofreading the manuscript, and his consent for acknowledgment has been obtained.

Author contributions
Asma Talebian: Methodology, investigation, data curation, writing–original draft. **Motahareh Soltani**: Investigation, data curation, writing–review & editing. **Somayyeh Karami-Mohajeri**: Supervision, project administration, methodology, formal analysis, writing–review & editing, funding acquisition. **Elham Jafari**: Investigation, validation, visualization, writing–review & editing. **Jafar Ahmadi**: Investigation, writing–original draft. **Mehdi Ranjbar**: Supervision, methodology, writing–review & editing. **Fatemeh Abedi**: writing–original draft. **Ali Mandegary**: writing–review & editing.

Funding
The project was supported by a grant (400000213) from the Pharmaceutics Research Center, Institute of Neuropharmacology, Kerman University of Medical Sciences, Kerman, Iran.

Declarations

Competing interests
The authors declare no competing interests.

Ethical approval
This study was approved by the Ethical Committee of Kerman University of Medical Sciences, Kerman, Iran (Ethic approval code: IR.KMU.REC.1400.362).

Additional information
Correspondence and requests for materials should be addressed to S.K.-M. or M.R.

Reprints and permissions information is available at www.nature.com/reprints.

Publisher's note Springer Nature remains neutral with regard to jurisdictional claims in published maps and institutional affiliations.

Open Access This article is licensed under a Creative Commons Attribution-NonCommercial-NoDerivatives 4.0 International License, which permits any non-commercial use, sharing, distribution and reproduction in any medium or format, as long as you give appropriate credit to the original author(s) and the source, provide a link to the Creative Commons licence, and indicate if you modified the licensed material. You do not have permission under this licence to share adapted material derived from this article or parts of it. The images or other third party material in this article are included in the article's Creative Commons licence, unless indicated otherwise in a credit line to the material. If material is not included in the article's Creative Commons licence and your intended use is not permitted by statutory regulation or exceeds the permitted use, you will need to obtain permission directly from the copyright holder. To view a copy of this licence, visit http://creativecommons.org/licenses/by-nc-nd/4.0/.

© The Author(s) 2025